

SLC37A2, a phosphorus-related molecule, increases in smooth muscle cells in the calcified aorta

Mariko Tani,¹ Sarasa Tanaka,¹ Chihiro Oeda,² Yuichi Azumi,¹ Hiromi Kawamura,¹ Motoyoshi Sakaue,¹ and Mikiko Ito^{1,*}

¹Graduate School of Human Science and Environment and ²School of Human Science and Environment, University of Hyogo, 1-1-12 Shinzaike-Honcho, Himeji, Hyogo 670-0092, Japan

(Received 26 November, 2019; Accepted 4 April, 2020; Published online 10 July, 2020)

Vascular calcification is major source of cardiovascular disease in patients with chronic kidney disease. Hyperphosphatemia leads to increased intracellular phosphorus influx, which leads to an increase in osteoblast-like cells in vascular smooth muscle cell. PiT-1 transports phosphate in vascular smooth muscle cell. However, the mechanism of vascular calcification is not completely understood. This study investigated candidate phosphorus-related molecules other than PiT-1. We hypothesized that phosphorus-related molecules belonging to the solute-carrier (SLC) superfamily would be involved in vascular calcification. As a result of DNA microarray analysis, we focused on SLC37A2 and showed that mRNA expression of these cells increased on calcified aortic smooth muscle cells (AoSMC). SLC37A2 has been reported to transport both glucose-6-phosphate/phosphate and phosphate/phosphate exchanges. *In vitro* analysis showed that SLC37A2 expression was not affected by inflammation on AoSMC. The expression of SLC37A2 mRNA and protein increased in calcified AoSMC. *In vivo* analysis showed that SLC37A2 mRNA expression in the aorta of chronic kidney disease rats was correlated with osteogenic marker genes. Furthermore, SLC37A2 was expressed at the vascular calcification area in chronic kidney disease rats. As a result, we showed that SLC37A2 is one of the molecules that increase with vascular calcification *in vitro* and *in vivo*.

Key Words: SLC37A2, vascular calcification, aortic smooth muscle cells, chronic kidney disease, hyperphosphatemia

As the number of patients with chronic kidney disease (CKD) increases, the number of patients requiring dialysis will increase as well. Most deaths in patients undergoing dialysis are due to cardiovascular disease such as cardiac failure, cerebrovascular disorders, or myocardial infarction.^(1,2) A major source of cardiovascular disease is ectopic calcification,⁽³⁾ an abnormality caused by the formation and deposition of calcium phosphate crystals in soft tissues.⁽⁴⁻⁶⁾ Various factors such as inflammation, oxidative stress, and increases in plasma calcium (Ca) and phosphorus (P) levels are involved in the progression of vascular calcification. Among these factors, hyperphosphatemia is most strongly associated with vascular calcification.^(7,8) Hyperphosphatemia is caused by excess intake of P in the presence of decreased renal function. Therefore, patients undergoing dialysis need to limit intake of P.^(7,9-12) However, it has been reported that vascular calcification is already progress when dialysis is started; it has also been seen in patients with early-stage CKD when hyperphosphatemia is not evident.⁽¹³⁾ Consequently, it is important to prevent vascular calcification in patients with early-stage CKD to improve life prognosis.

Vascular calcification is triggered by hyperphosphatemia,^(7,8)

which leads to an increased influx of P into vascular smooth muscle cells (VSMC). P influx is carried out via PiT-1, a transporter on the cell membrane surface of VSMC. PiT-1 is a member of the solute-carrier (SLC) superfamily, which includes a sodium phosphate transporter encoded by SLC20A1.⁽¹⁴⁾ PiT-1 transports phosphate across Na⁺-dependent cell membranes and subsequently promotes matrix mineralization due to elevated P levels.⁽¹⁵⁾ As intracellular P levels increase, VSMC begin to express osteogenic transcription factors, such as runt-related transcription factor 2 (Runx2).⁽¹⁶⁾ This effect is followed by increased expression of osteoblast-specific genes, such as osteopontin and osteocalcin. In addition, reduced expression of smooth muscle-specific proteins, such as smooth muscle protein 22- α (SM22- α), occurs. As a result, VSMC are transformed into osteoblast-like cells.^(17,18)

Recent clinical studies have shown that blood levels of calcium phosphate particles (CPP), which represent calcium phosphate colloidal particles, increase with decreasing renal function.⁽¹⁹⁻²¹⁾ Furthermore, correlations with blood CPP and P levels have been reported.^(20,21) It is possible that the CPP may trigger the progression of vascular calcification.⁽²²⁻²⁴⁾

However, vascular calcification has been observed in patients with early-stage CKD with normal plasma P levels.⁽¹³⁾ In addition, PiT-1 mRNA is expressed ubiquitously in all tissues. Thus another molecule may act primarily at the area of vascular calcification.

There are reports that inflammation promotes vascular calcification. Inflammatory factors such as interleukin (IL)-1 β , IL-6, and tumor necrosis factor- α (TNF- α) induced differentiation of VSMC into osteoblast-like cells.^(25,26) TNF- α induces vascular calcification through the cAMP pathway, which plays a role in osteoblast differentiation.^(27,28) IL-6 regulates various pathways leading to vascular calcification of VSMC.⁽²⁹⁻³¹⁾ Furthermore, IL-1 β , IL-6, and TNF- α are also factors associated with increased vascular calcification induced by high P levels.^(32,33) However, current data do not fully explain the mechanism of vascular calcification induced by these factors.

We hypothesized that there may be other P-related molecules, such as those in the SLC superfamily, involved in vascular calcification. We focused on membrane proteins in the SLC superfamily and investigated potential candidate P-related molecules other than PiT-1 for involvement in vascular calcification. Furthermore, we examined the relation between candidate molecules and vascular calcification *in vitro* and *in vivo*.

*To whom correspondence should be addressed.
E-mail: mito@shse.u-hyogo.ac.jp

Materials and Methods

Cell culture. Normal human aortic smooth muscle cells (AoSMC) were obtained from Lonza (Basel, Switzerland). AoSMC were cultured according to the manufacturer's instructions. AoSMC were maintained in growth medium (smooth muscle cell basal medium supplemented with 5% fetal bovine serum (FBS), epidermal growth factor, insulin, fibroblast growth factor-B, and gentamicin/amphotericin-B). Media were changed every other day. AoSMC were grown in a humidified 5% CO₂ incubator at 37°C and maintained until confluence was reached and then used in experiments.

Calcified AoSMC. Calcification of AoSMC was induced as described previously.^(34,35) AoSMC were cultured in Dulbecco's modified Eagle's medium supplemented with 15% FBS and penicillin-streptomycin and cultured with 2.6 mM P for 3, 6, 9, 12, and 14 days. The P concentration was adjusted by the P buffer (NaH₂PO₄/Na₂HPO₄, pH 7.2). Other AoSMC were not cultured with 2.6 mM P.

DNA microarray. Total RNA of AoSMC samples cultured and not cultured with 2.6 mM P were used. Total RNA 5.0 µg was analyzed using DNA microarray (Agilent Technologies, Tokyo, Japan). SurePrint G3 Human GE 8 × 60k ver. 2 Microarray was used to examine about 26,000 genes. The ratio was calculated by dividing the expression level on AoSMC cultured with 2.6 mM P for 12 days by the expression level on AoSMC non-cultured with 2.6 mM P.

Expression of SLC37A2 in vascular inflammation. To induce an inflammatory response in AoSMC, cells were cultured with growth medium until they reached confluence and then treated with 1 µg/mL lipopolysaccharides (LPS) (LPS from *Escherichia coli* O111:B4; Sigma, St. Louis, MO) for 24 and 72 h without 2.6 mM P. Other AoSMC were not cultured with LPS.

Real-time polymerase chain reaction (PCR) analysis. Total RNA was extracted from AoSMC treated with LPS for 24 and 72 h as well as cells not treated with LPS. SYBR green-based quantitative real-time PCR was performed using synthesized cDNA and an appropriate primer set for each target gene with a StepOnePlus real-time PCR system (Applied Biosystems, Foster City, CA). The primer sequences were as follows: human IL-6, 5'-AATTCGGTACATCCTCGACGG-3' and 5'-GCCATCTTTGGAAGTTTCAGG-3'; human SLC37A2, 5'-TCACCTTAGTGCCAAAGGAGG-3' and 5'-CCATTGGTGTAGTCAGAGACG-3'; glyceraldehyde-3-phosphate dehydrogenase (GAPDH), 5'-CTGCACCACCAACTGCTTAGC-3' and 5'-CTTCTGGGTGGCAGTGATGGC-3'. IL-6 and SLC37A2 mRNA expression levels were calculated after normalization with GAPDH.

Expression of SLC37A2 in calcified AoSMC. Total RNA were extracted from AoSMC not cultured with 2.6 mM P and AoSMC cells cultured with 2.6 mM P for 3, 6, 9, 12, and 14 days. Real-time PCR was performed using the synthesized cDNA. The primer sequences were as follows: human Runx2, 5'-TGAGAGCCGCTTCTCCAACCC-3' and 5'-CTCTGGCTTTGGGAAGAGCCG-3'. The Runx2 and SLC37A2 mRNA expression levels were calculated after normalization with GAPDH.

Western blotting analysis. Total protein was collected from AoSMC samples cultured under the same conditions used for real-time PCR analysis. These samples were lysed using Tris-buffered saline (pH 7.5) supplemented with 5% NP-40 and a 1% protease inhibitor cocktail. The protein concentration samples was measured using the BCA Protein Assay Kit (Thermo Fisher Scientific, Waltham, MA), and the concentration was adjusted. For western blotting, 10 µg of protein was separated in a 10% polyacrylamide gel using sodium dodecyl sulfate-polyacrylamide gel electrophoresis. The membrane was treated with SLC37A2 antibody (Novus Biologicals, Centennial, CO) or GAPDH antibody (GeneTex, Irvine, CA) as the primary antibodies, incubated with Rabbit IgG Horseradish peroxidase-conjugated antibody

(R&D Systems, Minneapolis, MN) as the secondary antibody, and visualized using Amersham ECL Select (GE Healthcare, Buckinghamshire, England) and luminescent image analyzer (LAS-1000 plus, FUJIFILM, Tokyo, Japan). The band was quantified using ImageJ.

Experimental protocols with adenine-induced CKD rats.

All study protocols were approved by the Ethics Committee of the University of Hyogo, School of Human Science and Environment. Twelve-week-old male, Sprague-Dawley rats were purchased from Japan SLC (Shizuoka, Japan). Rats were maintained on a 12-h light, 12-h dark cycle (09:00–21:00) and allowed free access to food and extra-pure water.

The experimental diets include a control P diet (1.0% P, 0.6% Ca, 20% protein), an adenine diet (0.75% adenine, 1.0% P, 0.6% Ca, 2.5% protein), a low-P (LP) diet (0.2% P, 0.6% Ca, 10% protein), and a high-P (HP) diet (1.0% P, 0.6% Ca, 10% protein) based on the AIN93-G diet (Oriental Yeast, Tokyo, Japan) with casein as the protein source.^(36,37) A low protein diet has been reported to promote vascular calcification in rats with adenine-induced renal failure, so protein restriction was performed.^(37,38) Before grouping, all rats ($n = 23$) were fed a standard MF diet (Oriental Yeast) for a week to acclimatize. At 13 weeks old, rats were divided into 2 groups: the control group ($n = 5$) and the adenine-induced CKD group ($n = 18$). The control group received the control P diet for 6 weeks. The adenine-induced CKD group received the adenine diet for about 3 weeks, and were then further divided into 2 subgroups: the CKD-LP group ($n = 8$) or the CKD-HP group ($n = 10$). Rats of the CKD-LP group and CKD-HP group received the LP diet and HP diet for 3 weeks, respectively. During the experimental period, food intake was recorded daily.

During the adenine diet, blood samples were collected from the tail vein between 10:00 AM and 11:00 AM once a week until the second week, and thereafter once every 2 days to monitor plasma P levels. During the LP-diet or HP-diet, blood samples were collected once a week. Urine samples were collected and urine volume was recorded once every week. Rats were sacrificed with anesthetic using isoflurane (Wako Pure Chemical Industries, Osaka Japan) and laparotomized. Blood samples taken from the inferior vena cava and thoracoabdominal aorta were collected for analysis.

Plasma and urine levels of P, Ca, and creatinine (Cr) were measured using the Wako Phospha-C test kit, the Wako Calcium-E test kit, and the Wako Creatinine test kit, respectively (Wako Pure Chemical Industries).

SLC37A2 expression on the aorta. Approximately one third of the collected thoracoabdominal aorta was used to visualize calcification and conduct immunostaining. The aorta was embedded in paraffin and 4-µm sections were cut. Sections were stained using a Von Kossa Method for Calcium Kit (Polysciences, Warrington, PA) according to the manufacturer's instructions. Immunostaining analysis was performed with serial sections. The sections were incubated with SLC37A2 antibody overnight at 4°C and then treated with Histofine Simple Stain Rat MAX-PO (MULTI) (Nichirei Biosciences, Tokyo, Japan) for 30 min at room temperature. Thereafter, sections were treated with a DAB substrate kit (Nichirei).

Total RNA was extracted from the rest of the frozen thoracoabdominal aorta. Real-time PCR was performed using the synthesized cDNA. The primer sequences were as follows: rat osteopontin, 5'-ACCCATCTCAGAAGCAGAATC-3' and 5'-ATC CATGTGGTCATGGCTTTC-3' and; rat SLC37A2, 5'-TAG TCCCAGCTTCGAGTACGG-3' and 5'-CTGATGGGCTTTCTG GACATG-3'. The osteopontin mRNA and SLC37A2 mRNA expression levels were calculated after normalization with GAPDH.

Statistical analysis. Data are presented as the mean ± SE. Differences between groups were analyzed using the *t* test. In phosphate-induced calcified AoSMC experiments, differences were analyzed using one-way analysis of variance followed by

Dunnett's method. In the CKD model rat experiments, differences were analyzed using the Kruskal-Wallis test followed by the Steel-Dwass method. Correlation coefficients (rs) were determined using Spearman's correlation coefficient rank test. For all tests, two-tailed *p* values <0.05 were considered statistically significant.

Results

Search for candidate molecules in phosphate-induced calcified AoSMC. To search for molecules whose expression increase in calcified AoSMC, DNA microarray analysis of about 26,000 genes was performed using calcified AoSMC and non-calcified AoSMC mRNA. Figure 1 shows the HeatMap of different genes expressed between AoSMC not cultured with 2.6 mM P and those cultured with 2.6 mM P for 12 days. A total of 3,066 genes increased more than two-fold on cultured vs non-cultured AoSMC. Genes with increased expression were molecules related to osteoblast formation such as osteopontin, periostin osteoblast specific factor (POSTN), Wnt3, interleukin-6 (IL-6), and fibroblast growth factor 23 (FGF23) as well as several molecules in the SLC superfamily (Table 1). Among these molecules, we focused on SLC37A2, for which mRNA increased about 3.1 times on AoSMC cultured with 2.6 mM P for 12 days compared to AoSMC not cultured with 2.6 mM P. SLC37A2 has been reported to be related to P regulation, but its detailed function is unknown.

Effect of inflammation on SLC37A2 expression. Vascular calcification has been reported to be promoted by inflammation, so we examined whether the SLC37A2 mRNA is affected by inflammatory response. At 24 h after LPS treatment, IL-6 mRNA significantly increased compared to AoSMC not treated with LPS (Fig. 2A). These results were also seen 72 h after LPS treatment. There were no significant differences between groups in SLC37A2 mRNA expression (Fig. 2B).

Expression of SLC37A2 in phosphate-induced calcified AoSMC. To determine whether SLC37A2 is involved in calcification, we examined the expression of SLC37A2 mRNA on non-calcified and calcified AoSMC (Fig. 3). Calcification was observed in AoSMC cultured with 2.6 mM P for 6 days, and more advanced calcification was observed in AoSMC cultured with 2.6 mM P for 12 days (Fig. 3A). Runx2 mRNA significantly increased on calcified AoSMC compared to non-calcified AoSMC (Fig. 3B). SLC37A2 mRNA significantly began to increase on day 3 in calcified AoSMC, and on day 9, calcified AoSMC significantly increased about two-fold compared with non-calcified AoSMC (Fig. 3C). Expression of SLC37A2 protein significantly increased about two-fold on day 6 in calcified AoSMC compared with non-calcified AoSMC (Fig. 3D).

Expression of SLC37A2 in CKD model rats. To reveal whether SLC37A2 involves in vascular calcification *in vivo*, we examined SLC37A2 mRNA expression on vessel of adenine-induced CKD rats. Adenine-induced CKD rats were created according to the protocol shown in Fig. 4A. Table 2 shows body weight and biochemical data on the day of sacrifice. Body weight of adenine-induced CKD rats was significantly lower compared with non-CKD rats. Compared with the non-CKD group, CKD groups had higher plasma P and Cr levels, and lower plasma Ca levels and 24-h urinary excretion of P, Ca, and Cr. Further, these results were more prominent in the CKD-HP group, as seen in previous studies.^(37,39) Thus, renal function decreased in the CKD group, particularly in the CKD-HP group.

We examined mRNA expression on aortic vessels of CKD rats (Fig. 4). Although there were no significant differences in expression of Runx2 mRNA, a transcription factor that moves early in the mechanism of vascular calcification, between groups (Fig. 4B), expression of osteopontin mRNA significantly increased in the CKD-HP group compared to non-CKD group and the CKD-LP group (Fig. 4C). SLC37A2 mRNA expression was also significantly increased in the CKD-HP group compared to the non-CKD

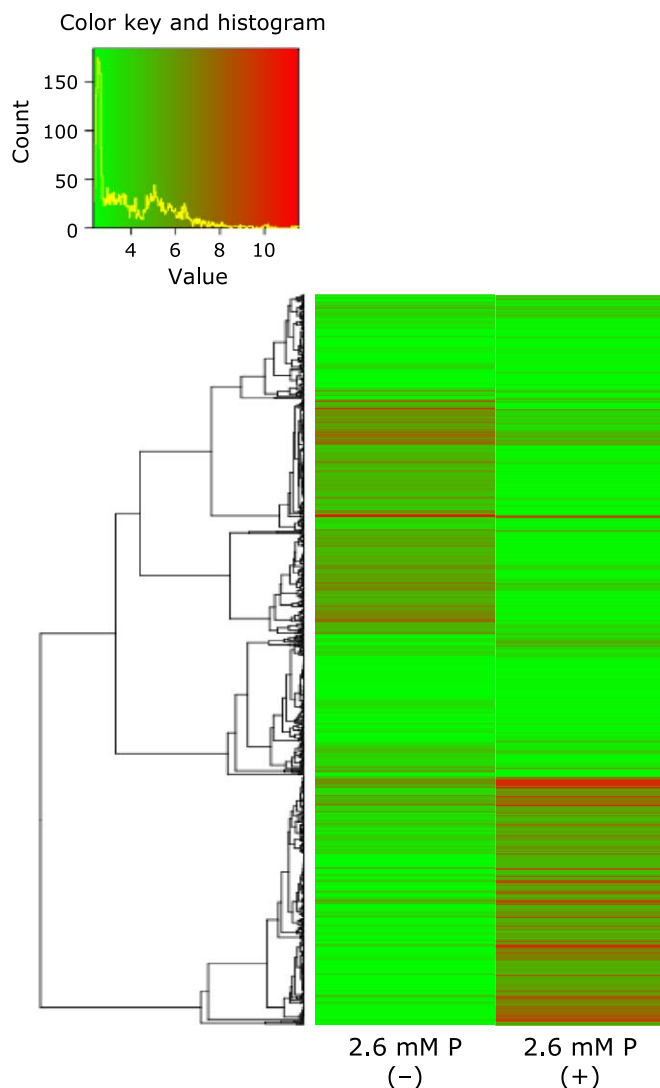


Fig. 1. The HeatMap of different expressed genes between AoSMC non-cultured with 2.6 mM P and AoSMC cultured with 2.6 mM P. Red represents genes with a high signal level, and green represents genes with a low signal level. AoSMC, aortic smooth muscle cells. See color figure in the on-line version.

Table 1. Increase in genes in aortic smooth muscle cells cultured with 2.6 mM phosphorus

Gene name	Ratio
Genes related to osteoblast formation	
Osteopontin	2.94
Periostin osteoblast specific factor	5.55
Wnt3	2.99
Interleukin 6	2.50
Fibroblast growth factor 23	2.83
Genes of SLC superfamily	
SLC12A7 (electroneutral potassium-chloride cotransporter)	2.55
SLC28A2 (sodium-dependent and purine-selective transporter)	6.34
SLC37A2 (P-linked glucose-6-phosphate antiporter)	3.11
SLC26A3 (chloride/bicarbonate exchanger)	2.72

The ratio was calculated by dividing the expression level on AoSMC cultured with 2.6 mM phosphorus for 12 days by the expression level on AoSMC non-cultured with 2.6 mM phosphorus.

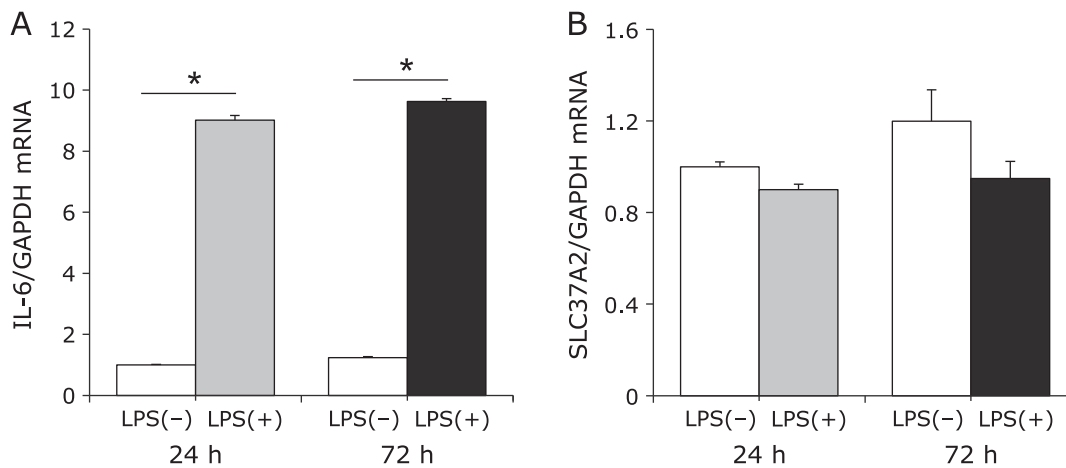


Fig. 2. Expression of SLC37A2 mRNA in AoSMC-induced inflammation. Total RNA was extracted from AoSMC treated with LPS for 24 and 72 h or not treated with LPS. Relative mRNA expression of (A) IL-6 and (B) SLC37A2 in AoSMC. Results are expressed as mean \pm SE. The level of each mRNA was normalized to that of glyceraldehyde-3-phosphate dehydrogenase mRNA. The mRNA expression level of AoSMC treated without LPS for 24 h was taken as 1. * $p < 0.01$. AoSMC, aortic smooth muscle cells; LPS, lipopolysaccharides; IL-6, interleukin 6.

group and CKD-LP group (Fig. 4D). Because there were large individual differences in these rats, we examined the correlation between osteopontin and SLC37A2 mRNA and found a significant correlation between these molecules (Fig. 4E).

Histological examination of the thoracoabdominal aorta revealed medial calcification only in the aorta of the CKD-HP group (Fig. 5A). To examine the expression site of SLC37A2 on the aorta, we conducted immunostaining of the aorta of CKD-HP rats. SLC37A2 was strongly expressed at the area where vascular calcification occurred (Fig. 5B).

Discussion

We investigated candidate P-related molecules involved in vascular calcification. Our results showed that SLC37A2 is one of the molecules that increase with vascular calcification *in vitro* and *in vivo*.

The SLC37 family belongs to the SLC superfamily and includes 4 proteins: SLC37A 1-4.⁽⁴⁰⁾ The SLC37 family contains transmembrane proteins in the endoplasmic reticulum membrane and has a sequence homologous to the bacterial organophosphate/phosphate antiporter.⁽⁴¹⁾ SLC37A4 is better known as the glucose-6-phosphate transporter.⁽⁴²⁻⁴⁴⁾ However, there are few reports about SLC37A2, and details about its function are not fully understood. SLC37A2, also known as SPX2, is abundantly expressed in murine macrophages, spleen, thymus, and white adipose tissue (WAT) of genetically obese mouse models and osteoclast-like cells derived from Raw264.7 cells.^(45,46) The SLC37A2 protein transports both glucose-6-phosphate/phosphate and phosphate/phosphate exchanges.⁽⁴¹⁾ Recently, reports have shown an association SLC37A2 with animal disease.⁽⁴⁷⁻⁴⁹⁾ An SLC37A2 defect causes craniomandibular osteopathy (CMO), a self-limiting proliferative bone disease, in terrier breeds.⁽⁴⁷⁾ In dairy cattle, an SLC37A2 homozygous mutation is responsible for embryonic death.^(48,49) In addition, SLC37A2 has been considered a target for vitamin D target genes.⁽⁵⁰⁾ The potential for the phospho-Ser294 progesterone receptor target gene in the progression of breast cancer has also been considered.⁽⁵¹⁾

It has been reported that inflammation may both cause and exacerbate vascular calcification.^(25,26) Furthermore, SLC37A2 is abundantly expressed in macrophages and WAT, which are affected by macrophage infiltration.⁽⁴⁵⁾ Therefore, we considered that SLC37A2 might be a molecule expressed during inflam-

mation. However, our findings showed no increase in SLC37A2 expression in AoSMC exposed to an inflammatory response. Thus, this molecule does not appear to be directly affected by inflammatory stimulation. It is possible that SLC37A2 may be involved in vascular calcification through a mechanism other than inflammation.

It has been reported that SLC37A2 acts as a P-linked antiporter.⁽⁴¹⁾ In addition, SLC37A2 was reported to be a target gene for vitamin D, and the SLC37A2 gene contains a major vitamin D receptor-binding site.^(50,52) Systematically correlated changes in the expression of SLC37A2 genes and circulating forms of vitamin D₃ have been seen in human peripheral blood mononuclear cells.⁽⁵⁰⁾ Vitamin D receptors bind to 1 α , 25-dihydroxyvitamin D₃, which is a metabolite of vitamin D₃, and regulate gene expression. 1 α , 25-dihydroxyvitamin D₃ functions in the absorption of Ca and P in the intestine, Ca mobilization in the bone, and reabsorption of Ca in the kidneys.⁽⁵³⁾ There is report that in adenine-induced CKD model rats, serum 1 α , 25-dihydroxyvitamin D₃ was significantly higher in rats of high-P diet intake, with advanced vascular calcification, compared to rats of low-P diet intake.⁽³⁹⁾ SLC37A2 may be related to P regulation via vitamin D. Further studies are needed to clarify that vitamin D effects on SLC37A2 expression *in vitro* and *in vivo*.

It has been shown that the mechanism of vascular calcification is similar to that of bone formation. The deficiency of SLC37A2 caused by CMO is clinically comparable to human infantile cortical hyperostosis, also known as Caffey disease.⁽⁴⁷⁾ In addition, there are reports that SLC37A2 is expressed in bone marrow and osteoclasts.⁽⁴⁶⁾ Hytton *et al.*⁽⁴⁷⁾ hypothesized that a dysfunction of SLC37A2 would cause an imbalance in the function of osteoblastic and osteoclastic bone formation, and as a result, lead to hyperostosis.

Runx2 is an essential transcription factor for vascular calcification. It is also reported that Runx2 is an osteoblast differentiation transcription factor expressed in developing breast epithelial cells.^(54,55) Runx2 appears to be necessary for the regulation of phospho-Ser294 progesterone target genes, which are associated with breast cancer progression. SLC37A2 is considered a candidate phospho-Ser294 progesterone receptor target gene.⁽⁵¹⁾ Therefore, it is considered that Runx2 may regulate SLC37A2. In the present study, the expression of SLC37A2 mRNA in the aorta of CKD rats was correlated with osteopontin mRNA, which a target gene of Runx2.

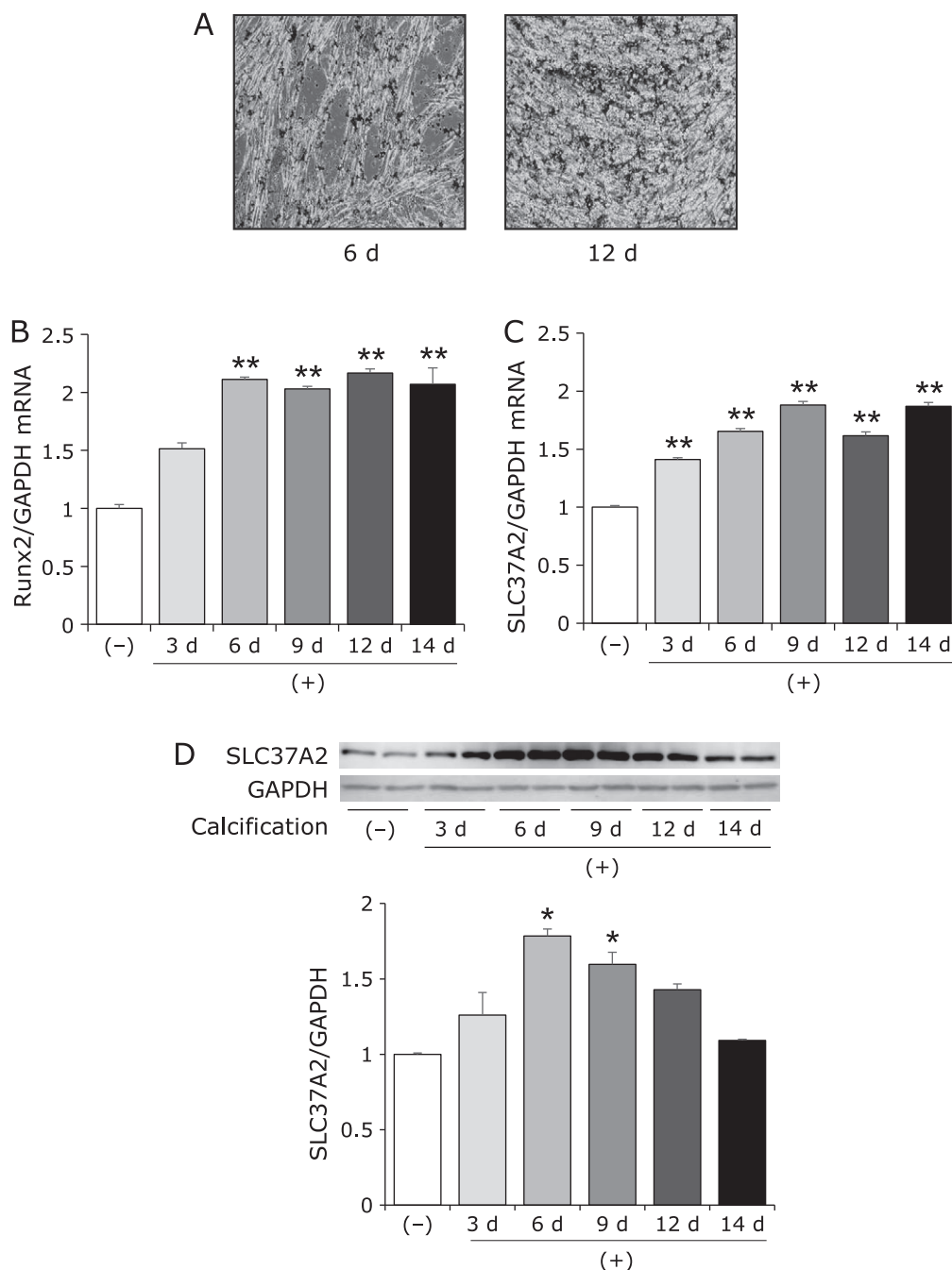


Fig. 3. Expression of SLC37A2 mRNA and protein in calcified AoSMC. (A) Von Kossa staining of AoSMC cultured with 2.6 mM P for 6 and 12 days. Relative mRNA expression of (B) Runx2 and (C) SLC37A2 in AoSMC. The level of each mRNA was normalized to that of glyceraldehyde-3-phosphate dehydrogenase mRNA. The mRNA expression level of non-calcified AoSMC was taken as 1. (D) The protein expression of SLC37A2 in AoSMC was determined by Western blot analysis. GAPDH was used as an internal control. (-) non-calcified; (+) calcified with 2.6 mM P for 3, 6, 9, 12, and 14 days. Results are expressed as mean \pm SE. * p <0.05, ** p <0.01 vs (-). AoSMC, aortic smooth muscle cells.

There are limitations in this study. First, we have shown that SLC37A2 may be the candidate molecules, but it remains unclear whether it is directly involved in vascular calcification. To clarify the function of SLC37A2, it is necessary to examine SLC37A2 gene knockdown and/or overexpression in AoSMC. However, AoSMC is very difficult cells to gene transfer because they are primary cells and insensitive to transfection reagents.⁽⁵⁶⁾ Therefore, there have been few reports of transfection into AoSMC.^(57,58) Furthermore, it is difficult to maintain the effect of gene transfer

for a long time because calcification takes about two weeks. Therefore, further studies are needed to clarify, such as the construction of a stable strain capable of controlling the expression of SLC37A2. Second, we conducted immunostaining of SLC37A2 on the aorta with vascular calcification *in vivo*, but did not examine the protein expression levels of whole aorta due to limited the amount of thoracoabdominal aorta that can be collected. Further studies are needed to clarify the differences in protein expression of SLC37A2 between groups, and the relation

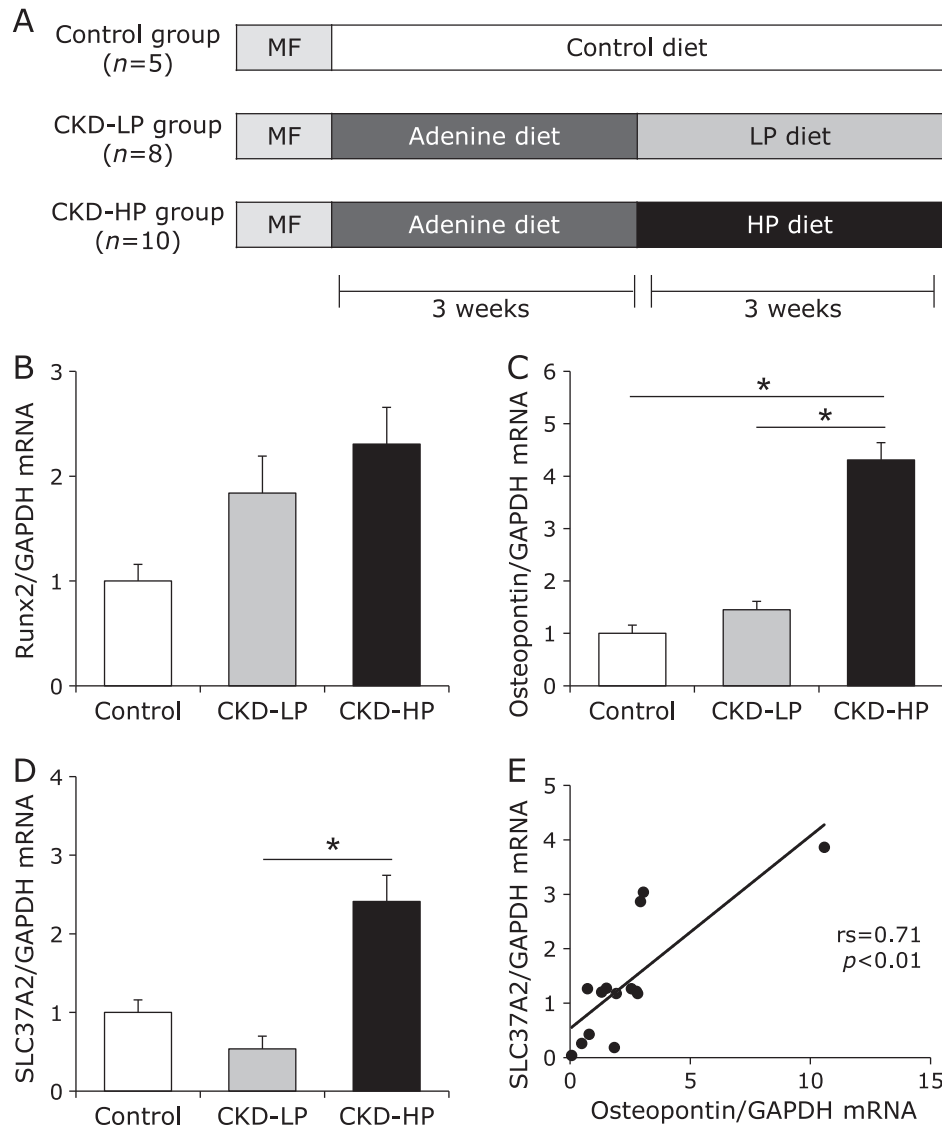


Fig. 4. Expression of calcification-related mRNA and SLC37A2 mRNA in the aorta of CKD rats. (A) Experimental design of adenine-induced CKD rats. Twelve-week-old male Sprague-Dawley rats were fed a standard MF diet for 1 week. At age 13 weeks, rats are divided into 2 groups: the control group and the adenine-induced CKD group. After about 3 weeks, the adenine-induced CKD group was divided into 2 subgroups: the CKD-LP group and the CKD-HP group for 3 weeks. CKD, chronic kidney disease; LP, low phosphorus; HP, high phosphorus. Relative mRNA expression of (B) Runx2, (C) osteopontin, and (D) SLC37A2 in the aorta. The mRNA expression level of the control group was taken as 1. (E) Correlation with SLC37A2 and osteopontin mRNA expression. The level of each mRNA was normalized to that of glyceraldehyde-3-phosphate dehydrogenase mRNA. Results are expressed as mean \pm SE. * p <0.05. CKD, chronic kidney disease; Runx2: runt-related transcription factor 2; rs, correlation coefficient.

Table 2. Body weight and biochemical data at sacrifice day

	Control	CKD-LP	CKD-HP
Body weight (g)	441.5 \pm 8.38	238.4 \pm 2.85**	217.4 \pm 5.16**,#
Plasma (mg/dl)			
P	5.49 \pm 0.18	3.74 \pm 0.29**	11.19 \pm 1.17*##
Ca	6.64 \pm 0.31	6.92 \pm 0.53	3.40 \pm 0.46**##
Cr	0.44 \pm 0.04	1.55 \pm 0.10**	0.96 \pm 0.05**##
Urine (mg/day)			
P	96.08 \pm 6.32	0.07 \pm 0.02**	43.44 \pm 4.15**##
Ca	0.22 \pm 0.09	0.03 \pm 0.02	0.01 \pm 0.01**
Cr	8.04 \pm 0.75	4.42 \pm 0.28*	3.47 \pm 0.44**

Values are mean \pm SE. * p <0.05 vs control group, ** p <0.01 vs control group, # p <0.05 vs CKD-LP group, ## p <0.01 vs CKD-LP group.

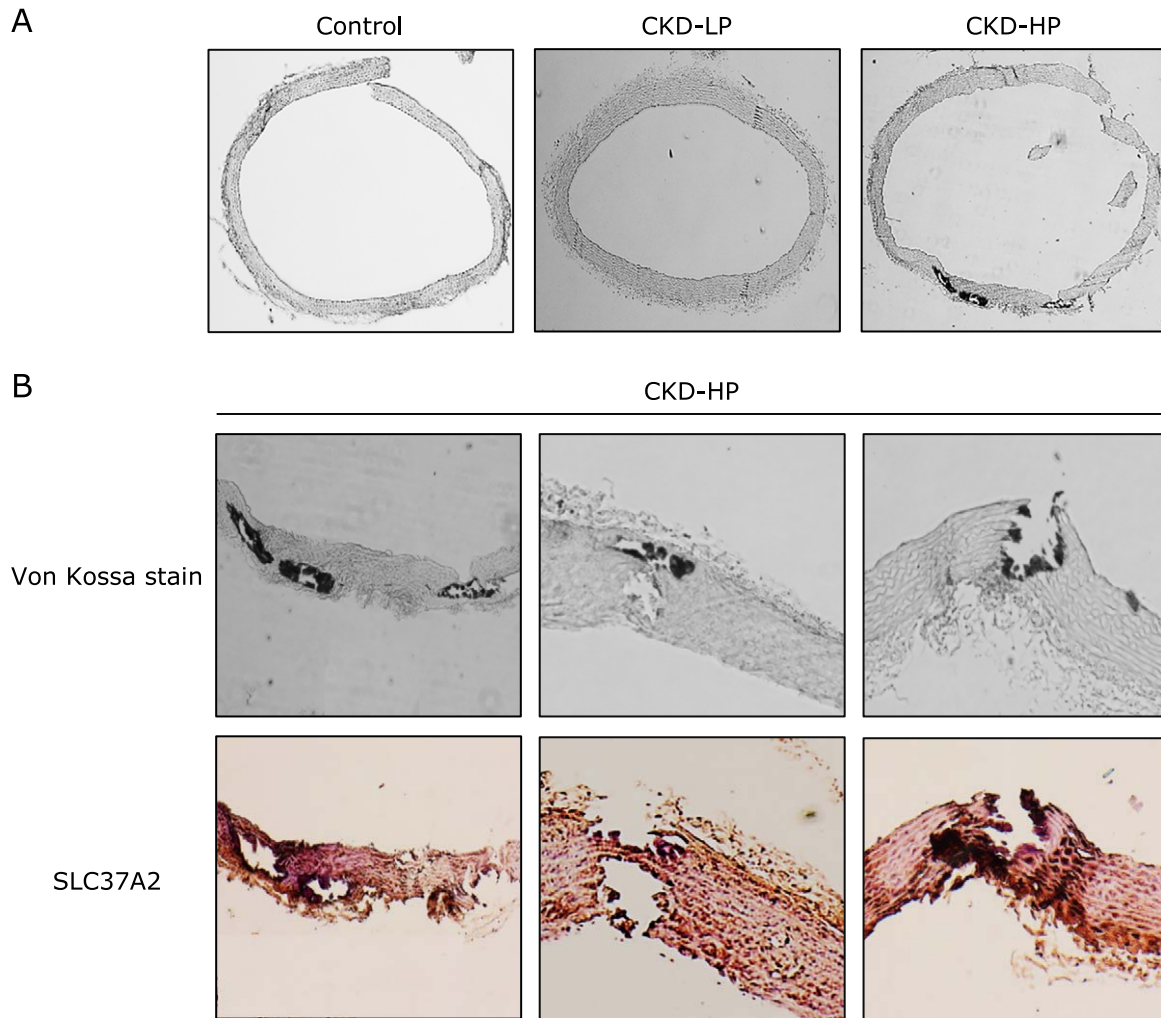


Fig. 5. Effects of dietary P on vascular calcification and location of SLC37A2 expression in the aorta. (A) Von Kossa staining of thoracoabdominal aorta in each group. (B) The upper panel is an enlarged figure of Von Kossa staining and the lower panel is SLC37A2 immunostaining of the thoracoabdominal aorta in the CKD-HP group. Original magnification: $\times 40$. P, phosphorus; CKD, chronic kidney disease; LP, low phosphorus; HP, high phosphorus.

between the degree of vascular calcification and SLC37A2 expression *in vivo*.

In conclusion, our findings indicate that SLC37A2 may be a molecule associated with the regulation of P and involved in vascular calcification via a pathway different to that seen with inflammation. Furthermore, SLC37A2 may be involved in vascular calcification as a factor downstream of Runx2. Our findings may provide new clues to elucidate the mechanism of P-induced vascular calcification. Further studies are needed to elucidate the function of SLC37A2 in relation to calcification.

Acknowledgments

This study was supported in part by a Grant-in-Aid for Scientific Research (C) from the Japan Society for the Promotion for Science (JSPS KAKENHI No. 17K00868).

Abbreviations

AoSMC aortic smooth muscle cells
Ca calcium
CKD chronic kidney disease

CMO craniomandibular osteopathy
CPP calciprotein particles
Cr creatinine
GAPDH glyceraldehyde-3-phosphate dehydrogenase
IL Interleukin
LPS lipopolysaccharides
P phosphorus
Runx2 runt-related transcription factor 2
SLC solute-carrier
TNF- α tumor necrosis factor-alpha
VSMC vascular smooth muscle cells
WAT white adipose tissue

Conflict of Interest

No potential conflicts of interest were disclosed.

References

- Go AS, Chertow GM, Fan D, McCulloch CE, Hsu CY. Chronic kidney disease and the risks of death, cardiovascular events, and hospitalization. *N Engl J Med* 2004; **351**: 1296–1305.
- London GM, Guérin AP, Marchais SJ, Métivier F, Pannier B, Adda H. Arterial media calcification in end-stage renal disease: impact on all-cause and cardiovascular mortality. *Nephrol Dial Transplant* 2003; **18**: 1731–1740.
- Cozzolino M, Brancaccio D, Gallieni M, Slatopolsky E. Pathogenesis of vascular calcification in chronic kidney disease. *Kidney Int* 2005; **68**: 429–436.
- Chavkin NW, Chia JJ, Crouthamel MH, Giachelli CM. Phosphate uptake-independent signaling functions of the type III sodium-dependent phosphate transporter, PiT-1, in vascular smooth muscle cells. *Exp Cell Res* 2015; **333**: 39–48.
- Shanahan CM, Crouthamel MH, Kapustin A, Giachelli CM. Arterial calcification in chronic kidney disease: key roles for calcium and phosphate. *Circ Res* 2011; **109**: 697–711.
- Yamada S, Giachelli CM. Vascular calcification in CKD-MBD: roles for phosphate, FGF23, and Klotho. *Bone* 2017; **100**: 87–93.
- Block GA, Klassen PS, Lazarus JM, Ofsthun N, Lowrie EG, Chertow GM. Mineral metabolism, mortality, and morbidity in maintenance hemodialysis. *J Am Soc Nephrol* 2004; **15**: 2208–2218.
- Taniguchi M, Fukagawa M, Fujii N, et al.; Committee of Renal Data Registry of the Japanese Society for Dialysis Therapy. Serum phosphate and calcium should be primarily and consistently controlled in prevalent hemodialysis patients. *Ther Apher Dial* 2013; **17**: 221–228.
- Taketani Y, Koiwa F, Yokoyama K. Management of phosphorus load in CKD patients. *Clin Exp Nephrol* 2017; **21** (Suppl 1): 27–36.
- Block GA, Port FK. Re-evaluation of risks associated with hyperphosphatemia and hyperparathyroidism in dialysis patients: recommendations for a change in management. *Am J Kidney Dis* 2000; **35**: 1226–1237.
- Ganesh S, Stack A, Levin N, Hulbert-Shearon T, Port F. Association of elevated serum PO₄, Ca x PO₄ product, and parathyroid hormone with cardiac mortality risk in chronic hemodialysis patients. *J Am Soc Nephrol* 2001; **12**: 2131–2138.
- Japanese Society of Nephrology. Dietary recommendations for chronic kidney disease, 2014. *Nihon Jinzo Gakkai Shi* 2014; **56**: 553–599. (in Japanese)
- Benz K, Varga I, Neureiter D, et al. Vascular inflammation and media calcification are already present in early stages of chronic kidney disease. *Cardiovasc Pathol* 2017; **27**: 57–67.
- Forster IC, Hernando N, Biber J, Murer H. Phosphate transporters of the SLC20 and SLC34 families. *Mol Aspects Med* 2013; **34**: 386–395.
- Jono S, McKee M, Murry C, et al. Phosphate regulation of vascular smooth muscle cell calcification. *Circ Res* 2000; **87**: E10–E17.
- Shao JS, Cai J, Towler DA. Molecular mechanisms of vascular calcification: lessons learned from the aorta. *Arterioscler Thromb Vasc Biol* 2006; **26**: 1423–1430.
- Giachelli CM, Speer MY, Li X, Rajachar RM, Yang H. Regulation of vascular calcification: roles of phosphate and osteopontin. *Circ Res* 2005; **96**: 717–722.
- Demer LL, Tintut Y. Vascular calcification: pathobiology of a multifaceted disease. *Circulation* 2008; **117**: 2938–2948.
- Miura Y, Iwazu Y, Shiizaki K, et al. Identification and quantification of plasma calciprotein particles with distinct physical properties in patients with chronic kidney disease. *Sci Rep* 2018; **8**: 1256.
- Smith ER, Ford ML, Tomlinson LA, Rajkumar C, McMahon LP, Holt SG. Phosphorylated fetuin-A-containing calciprotein particles are associated with aortic stiffness and a procalcific milieu in patients with pre-dialysis CKD. *Nephrol Dial Transplant* 2012; **27**: 1957–1966.
- Hamano T, Matsui I, Mikami S, et al. Fetuin-mineral complex reflects extraosseous calcification stress in CKD. *J Am Soc Nephrol* 2010; **21**: 1998–2007.
- Viegas CSB, Santos L, Macedo AL, et al. Chronic kidney disease circulating calciprotein particles and extracellular vesicles promote vascular calcification: a role for GRP (Gla-rich protein). *Arterioscler Thromb Vasc Biol* 2018; **38**: 575–587.
- Aghagolzadeh P, Radpour R, Bachtler M, et al. Hydrogen sulfide attenuates calcification of vascular smooth muscle cells via KEAP1/NRF2/NQO1 activation. *Atherosclerosis* 2017; **265**: 78–86.
- Aghagolzadeh P, Bachtler M, Bijarnia R, et al. Calcification of vascular smooth muscle cells is induced by secondary calciprotein particles and enhanced by tumor necrosis factor- α . *Atherosclerosis* 2016; **251**: 404–414.
- Liu J, Ma KL, Gao M, et al. Inflammation disrupts the LDL receptor pathway and accelerates the progression of vascular calcification in ESRD patients. *PLoS One* 2012; **7**: e47217.
- Ruiz-Andres O, Sanchez-Niño MD, Moreno JA, et al. Downregulation of kidney protective factors by inflammation: role of transcription factors and epigenetic mechanisms. *Am J Physiol Renal Physiol* 2016; **311**: F1329–F1340.
- Tintut Y, Patel J, Parhami F, Demer L. Tumor necrosis factor- α promotes *in vitro* calcification of vascular cells via the cAMP pathway. *Circulation* 2000; **102**: 2636–2642.
- Tintut Y, Parhami F, Boström K, Jackson S, Demer L. cAMP stimulates osteoblast-like differentiation of calcifying vascular cells. Potential signaling pathway for vascular calcification. *J Biol Chem* 1998; **273**: 7547–7553.
- Sun M, Chang Q, Xin M, Wang Q, Li H, Qian J. Endogenous bone morphogenetic protein 2 plays a role in vascular smooth muscle cell calcification induced by interleukin 6 *in vitro*. *Int J Immunopathol Pharmacol* 2017; **30**: 227–237.
- Callegari A, Coons ML, Ricks JL, Rosenfeld ME, Scatena M. Increased calcification in osteoprotegerin-deficient smooth muscle cells: dependence on receptor activator of NF- κ B ligand and interleukin 6. *J Vasc Res* 2014; **51**: 118–131.
- Abedin M, Lim J, Tang TB, Park D, Demer LL, Tintut Y. N-3 fatty acids inhibit vascular calcification via the p38-mitogen-activated protein kinase and peroxisome proliferator-activated receptor- γ pathways. *Circ Res* 2006; **98**: 727–729.
- Voelkl J, Lang F, Eckardt KU, et al. Signaling pathways involved in vascular smooth muscle cell calcification during hyperphosphatemia. *Cell Mol Life Sci* 2019; **76**: 2077–2091.
- Zhang D, Bi X, Liu Y, et al. High phosphate-induced calcification of vascular smooth muscle cells is associated with the TLR4/NF- κ B signaling pathway. *Kidney Blood Press Res* 2017; **42**: 1205–1215.
- Son BK, Akishita M, Iijima K, et al. Adiponectin antagonizes stimulatory effect of tumor necrosis factor- α on vascular smooth muscle cell calcification: regulation of growth arrest-specific gene 6-mediated survival pathway by adenosine 5'-monophosphate-activated protein kinase. *Endocrinology* 2008; **149**: 1646–1653.
- Son BK, Kozaki K, Iijima K, et al. Gas6/Axl-PI3K/Akt pathway plays a central role in the effect of statins on inorganic phosphate-induced calcification of vascular smooth muscle cells. *Eur J Pharmacol* 2007; **556**: 1–8.
- Nakahashi O, Yamamoto H, Tanaka S, et al. Short-term dietary phosphate restriction up-regulates ileal fibroblast growth factor 15 gene expression in mice. *J Clin Biochem Nutr* 2014; **54**: 102–108.
- Yamada S, Tokumoto M, Tatsumoto N, Tsuruya K, Kitazono T, Ooboshi H. Very low protein diet enhances inflammation, malnutrition, and vascular calcification in uremic rats. *Life Sci* 2016; **146**: 117–123.
- Price PA, Roublick AM, Williamson MK. Artery calcification in uremic rats is increased by a low protein diet and prevented by treatment with ibandronate. *Kidney Int* 2006; **70**: 1577–1583.
- Yamada S, Tokumoto M, Tatsumoto N, et al. Phosphate overload directly induces systemic inflammation and malnutrition as well as vascular calcification in uremia. *Am J Physiol Renal Physiol* 2014; **306**: F1418–F1428.
- Cappello AR, Curcio R, Lappano R, Maggiolini M, Dolce V. The physiological role of the exchangers belonging to the SLC37 family. *Front Chem* 2018; **6**: 122.
- Pan CJ, Chen SY, Jun HS, Lin SR, Mansfield BC, Chou JY. SLC37A1 and SLC37A2 are phosphate-linked, glucose-6-phosphate antiporters. *PLoS One* 2011; **6**: e23157.
- Pan C, Lin B, Chou J. Transmembrane topology of human glucose 6-phosphate transporter. *J Biol Chem* 1999; **274**: 13865–13869.
- Chen SY, Pan CJ, Nandigama K, Mansfield BC, Ambudkar SV, Chou JY. The glucose-6-phosphate transporter is a phosphate-linked antiporter deficient in glycogen storage disease type Ib and Ic. *FASEB J* 2008; **22**: 2206–2213.
- Pan CJ, Chen SY, Lee S, Chou JY. Structure-function study of the glucose-6-phosphate transporter, an eukaryotic antiporter deficient in glycogen storage disease type Ib. *Mol Genet Metab* 2009; **96**: 32–37.
- Kim JY, Tillison K, Zhou S, Wu Y, Smas CM. The major facilitator superfamily member Slc37a2 is a novel macrophage-specific gene selectively expressed in obese white adipose tissue. *Am J Physiol Endocrinol Metab*

- 2007; **293**: E110–E120.
- 46 Ha BG, Hong JM, Park JY, *et al.* Proteomic profile of osteoclast membrane proteins: identification of Na⁺/H⁺ exchanger domain containing 2 and its role in osteoclast fusion. *Proteomics* 2008; **8**: 2625–2639.
- 47 Hytönen MK, Arumilli M, Lappalainen AK, *et al.* Molecular characterization of three canine models of human rare bone diseases: Caffey, van den Ende-Gupta, and Raine syndromes. *PLoS Genet* 2016; **12**: e1006037.
- 48 Reinartz S, Distl O. Validation of deleterious mutations in vorderwald cattle. *PLoS One* 2016; **11**: e0160013.
- 49 Fritz S, Capitan A, Djari A, *et al.* Detection of haplotypes associated with prenatal death in dairy cattle and identification of deleterious mutations in GART, SHBG and SLC37A2. *PLoS One* 2013; **8**: e65550.
- 50 Saksa N, Neme A, Rynänen J, *et al.* Dissecting high from low responders in a vitamin D3 intervention study. *J Steroid Biochem Mol Biol* 2015; **148**: 275–282.
- 51 Knutson TP, Truong TH, Ma S, *et al.* Posttranslationally modified progesterone receptors direct ligand-specific expression of breast cancer stem cell-associated gene programs. *J Hematol Oncol* 2017; **10**: 89.
- 52 Wilfinger J, Seuter S, Tuomainen TP, *et al.* Primary vitamin D receptor target genes as biomarkers for the vitamin D3 status in the hematopoietic system. *J Nutr Biochem* 2014; **25**: 875–884.
- 53 DeLuca H. Overview of general physiologic features and functions of vitamin D. *Am J Clin Nutr* 2004; **80** (6 Suppl): 1689S–1696S.
- 54 Ferrari N, McDonald L, Morris JS, Cameron ER, Blyth K. RUNX2 in mammary gland development and breast cancer. *J Cell Physiol* 2013; **228**: 1137–1142.
- 55 McDonald L, Ferrari N, Terry A, *et al.* RUNX2 correlates with subtype-specific breast cancer in a human tissue microarray, and ectopic expression of Runx2 perturbs differentiation in the mouse mammary gland. *Dis Model Mech* 2014; **7**: 525–534.
- 56 Nabzdyk CS, Chun M, Pradhan L, Logerfo FW. High throughput RNAi assay optimization using adherent cell cytometry. *J Transl Med* 2011; **9**: 48.
- 57 Nabzdyk CS, Chun MC, Oliver-Allen HS, *et al.* Gene silencing in human aortic smooth muscle cells induced by PEI-siRNA complexes released from dip-coated electrospun poly(ethylene terephthalate) grafts. *Biomaterials* 2014; **35**: 3071–3079.
- 58 Shukla S, Fujita K, Xiao Q, Liao Z, Garfield S, Srinivasula SM. A shear stress responsive gene product PP1201 protects against Fas-mediated apoptosis by reducing Fas expression on the cell surface. *Apoptosis* 2011; **16**: 162–173.



This is an open access article distributed under the terms of the Creative Commons Attribution-NonCommercial-NoDerivatives License (<http://creativecommons.org/licenses/by-nc-nd/4.0/>).
